AIChE Letter: Inorganic Materials: Synthesis and Processing

Co-firing Technology for the Preparation of Asymmetric Oxygen Transporting Membranes based on BSCF and Zr-doped BSCF

U. Pippardt, J. Böer, L. Kiesel, R. Kircheisen, R. Kriegel, and I. Voigt
Fraunhofer Institute for Ceramic Technologies and Systems IKTS, Michael-Faraday-Str. 1, D-07629, Hermsdorf, Germany

DOI 10.1002/aic.14283
Published online November 19, 2013 in Wiley Online Library (wileyonlinelibrary.com)

Significance

Asymmetric tubular membranes with a length of 450 mm were prepared in one step by co-firing of a green support coated by slurry. BSCF ($Ba_{0.5}Sr_{0.5}Co_{0.8}Fe_{0.2}O_{3-\delta}$) and Zr-doped BSCF3Zr ($Ba_{0.5}Sr_{0.5}(Co_{0.8}Fe_{0.2})_{0.97}Zr_{0.03}O_{3-\delta}$) were used for the separation layer as well as for the porous support, latter one together with PMMA microspheres as a pore forming agent. The gas leakage at room temperature was below 0.003 mL STP/(cm²·min). Oxygen fluxes up to 12 mL STP/(cm²·min) were observed at 900°C in vacuo *operation mode. The oxygen flux increased with growing driving force but the slope of the curve flattened at higher driving forces probably caused by limiting surface exchange and pressure losses inside the porous support. The oxygen permeation of asymmetric BSCF tubes was slightly higher compared to BSCF3Zr and exceeded the oxygen flux of a monolithic BSCF membrane by a factor of 4 at comparable operation conditions.* © 2013 American Institute of Chemical Engineers *AIChE J*, 60: 15–21, 2014

Keywords: gas purification, membrane materials, membrane separations

Introduction

Oxygen separation from air is still an issue due to the fact that oxygen is the mostly used reactant in chemical and combustion processes. The cryogenic oxygen separation is well established but too expensive for most of the combustion and oxidation processes. Therefore, the development of oxygen selective membranes is favored with a clear focus on reduced separation costs.

Ceramic membranes with a mixed conductivity of oxygen ions as well as electrons for high-temperature oxygen separation were already proposed 25 years ago by Teraoka et al.[1] followed by a period of optimizing the composition to maximize the oxygen permeation as well as the stability.[2] $Ba_{0.5}Sr_{0.5}Co_{0.8}Fe_{0.2}O_{3-\delta}$ (BSCF) was found to be one of the most promising materials.[3] Tubular membrane samples with a thickness of 1.7 mm showed an oxygen permeation in the range of 3 mL STP/(cm^2·min) in an oxygen partial pressure gradient 0.21/0.01 at a temperature of 850°C. However, long-term tests combined with a careful investigation of the phase composition indicated structural instability of BSCF. Below 850°C, the desired cubic perovskite is transformed into a hexagonal phase.[4,5] The stability could be improved by partial substitution of B-cations with bigger cations like niobium[6] or zirconium.[7] Besides, BSCF and BSCF3Zr possess high-creeping rates as well as a high-chemical expansion. Therefore, the approach of stacks built-up of flat membranes favored by Air Products[8] seems to be not meaningful. This approach needs perovskite compositions with lower expansion and lower creeping rates usually entailed by lower oxygen permeation as well.

Nevertheless, stable long-term operation of tubular BSCF membranes was proven for a stand-alone oxygen generator equipped with a membrane area of 0.2 m^2 (19 monochannel tubes) realizing an oxygen permeation of ≈ 1.4 mL STP/(cm^2·min) 850°C.[9,10] The device used ambient air on the feed side and vacuum on the permeate side.

A distinct increase of the oxygen permeation should be possible by smaller membrane thickness. A promising possibility is the preparation of thin membrane layers on top of a porous support. Due to the high-thermal expansion combined with a remarkable chemical expansion, a support from the same composition is favored. The coating and final densification of the membrane layer on top of a sintered support

Correspondence concerning this article should be addressed to U. Pippardt at ute.pippardt@ikts.fraunhofer.de.

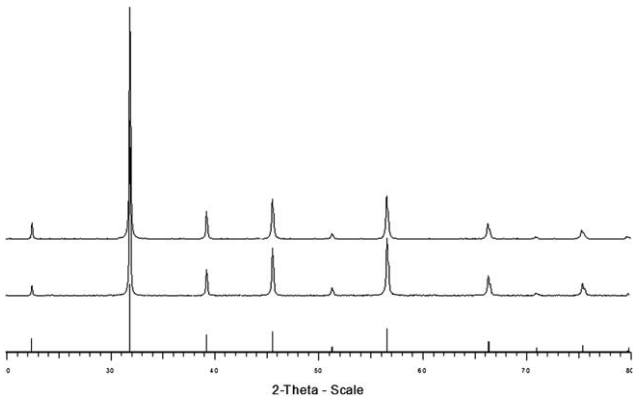

Figure 1. XRD measurements of raw powders $Ba_{0.5}Sr_{0.5}Co_{0.8}Fe_{0.2}O_{3-\delta}$ (BSCF) and $Ba_{0.5}Sr_{0.5}(Co_{0.8}Fe_{0.2})_{0.97}Zr_{0.03}O_{3-\delta}$ (BSCF3Zr).

requires a multistep coating with individual sintering. Schulz et al.[11] reported about five different coating steps including dip coating, paste coating and electrophoresis combined with intermediate sintering on porous BSCF tubes. The membrane tubes manufactured as described were characterized by an open porosity of 31 vol. %, a mean pore size of 6 μm and a leakage rate of 0.08 mL(STP)/(cm^2·min).

It seems to be clear that a competitive production of asymmetric membranes requires a one-step coating together with one step sintering. A promising approach is based on the usage of the sintering shrinkage of the support to densify the membrane layer. Accordingly, Norsk Hydro prepared La_2NiO_4 membranes on presintered La_2NiO_4 supports containing a bimodal pore-size distribution.[12] During sintering the fraction of small pores was densified at first entailed by a partial shrinkage of the support combined with the sintering of the membrane layer. The porosity of the support could be reached by the addition of additives (pore formers) to the ceramic body which burn off during sintering. Kovalevsky et al.[13] prepared thin BSCF membranes on hydrostatic pressed BSCF supports using graphite as a pore former. Schulze-Küppers prepared thin BSCF membranes on top of porous BSCF discs by tape casting using different types of starch as pore former.[14] In contrast to tape casting, extrusion of membrane tubes is characterized by high compression and shear forces resulting in a deformation of weak pore formers like starch or graphite. Therefore, pores shaped like slits and aligned along the extrusion direction will be obtained. Moreover, these pores are oriented perpendicular to the direction of the oxygen permeation.

According to overcome the drawbacks of this state of the art, this article reports the preparation of tubular BSCF as well as BSCF3Zr supports using PMMA spheres as pore formers and the preparation of dense membranes by a one-step coating and cofiring.

Experimental

Preparation

Powder. Undoped and Zr-doped BSCF ($Ba_{0.5}Sr_{0.5}Co_{0.8}Fe_{0.2}O_{3-\delta}$) powder delivered by Treibacher Industrie AG Austria (TIAG) were used. The chemical compositions $Ba_{0.5}Sr_{0.5}Co_{0.8}Fe_{0.2}O_{3-\delta}$ (BSCF) and $Ba_{0.5}Sr_{0.5}(Co_{0.8}Fe_{0.2})_{0.97}Zr_{0.03}O_3$ (BSCF3Zr) correspond to a substitution degree of $x = 0$ and $x = 0.03$ of a general chemical composition $Ba_{0.5}Sr_{0.5}(Co_{0.8}Fe_{0.2})_{1-x}Zr_xO_{3-\delta}$. According to the XRD measurements depicted in Figure 1, both powders consisted of a pure cubic perovskite phase only. No hints for earth alkaline carbonates or free zirconia were observed. The average particle size amounted 2.7 μm for BSCF and 1.6 μm for BSCF3Zr, the specific surface area was 1.39 m^2/g and 1.80 m^2/g, respectively. Both powders were used for the manufacturing of the porous supports as well as for the coating.

Support. Porous supports were prepared by stiff-plastic extrusion of ceramic powders mixed with 20 wt % of PMMA Spheromeres® CA15 delivered by microbeads AG. Hydroxypropyl methylcellulose by DOW Chemical was used as binder together with methyl hydroxypropylcellulose produced by HERCULES. The powder, the pore forming agent and the binder were mixed with water using a BRABENDER® Plasti-Corder® Lab-Station7 equipped with a mixer type 350. The mixed batches were extruded into tubes using a BRABENDER® Plasti-Corder® Lab-Station7 extruder cascade together with an extrusion die characterized by an outer diameter of 12.25 mm and an inner diameter of 9.75 mm. The tubes extruded were dried at ambient conditions for 24 h. Figure 2 shows a SEM picture of the cross section of a dried BSCF3Zr tube containing PMMA microspheres.

Sample Preparation for Dilatometer Measurement. The preparation of asymmetric membranes by co-firing requires a characterization and adaptation of the different shrinkage of the coating layer and the support. The shrinkage of the support was measured by dilatometry using a piece of a dried support cut into a half tube segment with a length of 20 mm. The samples representing the membrane layer were prepared by uniaxial compaction of dry powders using a screw press applying a low pressure of 0.6 MPa. The compressed pellets possessed a diameter of 5 mm and length of 10 mm. Shrinkage measurements were carried out using a TMA 92-16.18 apparatus by SETARAM.

Dense Asymmetric Membranes. Coating of supports was carried out using a slurry with a viscosity of $\approx$ 2000 mPas.

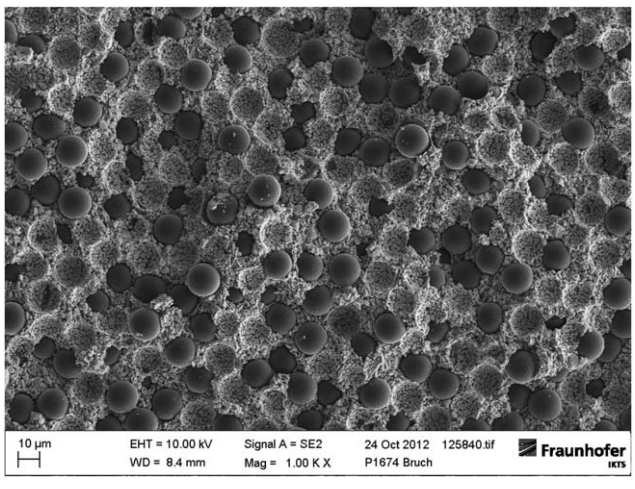

Figure 2. SEM picture of the cross section of a dried BSCF3Zr support tube containing PMMA microspheres.

Figure 3. Picture of the prepared asymmetric membrane with a length of ≈ 420 mm.

[Color figure can be viewed in the online issue, which is available at wileyonlinelibrary.com.]

The powders of BSCF and BSCF3Zr were mixed with terpineol (isomeric mixture, Merck), with a mixture of two binders (ethylcellulose, 5–15 mPa·s, and 30–60 mPa·s, SIGMA Life Science), and with a plasticizer (polyethylene glycol 1000, Merck) in a ball mill for 2 h. The solid content of the as-prepared slurry was 75 wt %. The membrane layer was coated onto the outside of the green supports by a conventional dip coating process. Coated membranes were dried for 24 h at room temperature and afterwards co-fired at 1100°C for 2 h in air. A critical preparation step was the burning out of the binder. The corresponding process was decelerated by a very low-heating rate of 1 K/min in the temperature range between 20 and 500°C. Asymmetric membrane tubes with a length of 450 mm and an outer diameter of 10 mm were obtained according to Figure 3.

Measurements

Leakage rate. The leakage rate of the sintered asymmetric membranes was determined using a purpose-built test bench. The membrane sample was clamped and sealed at the open tube ends followed by evacuation using a vacuum pump. The evacuated volume was separated from the pump by closing of a magnetic valve and the pressure inside the evacuated space was measured for 2 min. The increase of the vacuum pressure with time was used to calculate the absolute leakage rate by means of the total evacuated volume. The absolute leakage rate obtained was afterwards normalized to the membrane surface.

Oxygen Permeation. Oxygen permeation was measured in a testing device related to equipment already described by Schulz et al.[11] A membrane tube with a length of about 420 mm was fixed in an electrical furnace with a total length of 300 mm. The upper open end of the membrane tube was closed and permeated oxygen was withdrawn at the lower open end of the membrane by a vacuum pump. The gas-tight connection of the membrane tube to the vacuum system was realized by a vacuum tight adapter (Typ FE by WEH GmbH). The temperature profile along the membrane was measured using a thermocouple inside the membrane tube. The scheme of the testing device and the temperature profile measured are depicted in Figure 4. The nominal membrane length contributing to the total oxygen flux was estimated to 94 mm based on the temperature profile resulting in a nominal working membrane surface of 29.5 cm^2 for the asymmetric membrane tubes.[19] The vacuum pressure was determined by pressure sensors at both ends of the membrane located nearby the sealing area. The inner diameter of the vacuum piping was higher than the inner diameter of the membrane to prevent pressure drops inside the piping.

Oxygen permeation measurements were carried out between 700 and 900°C using a steps of 50 K. At each step the temperature was held constant and the vacuum pressure was

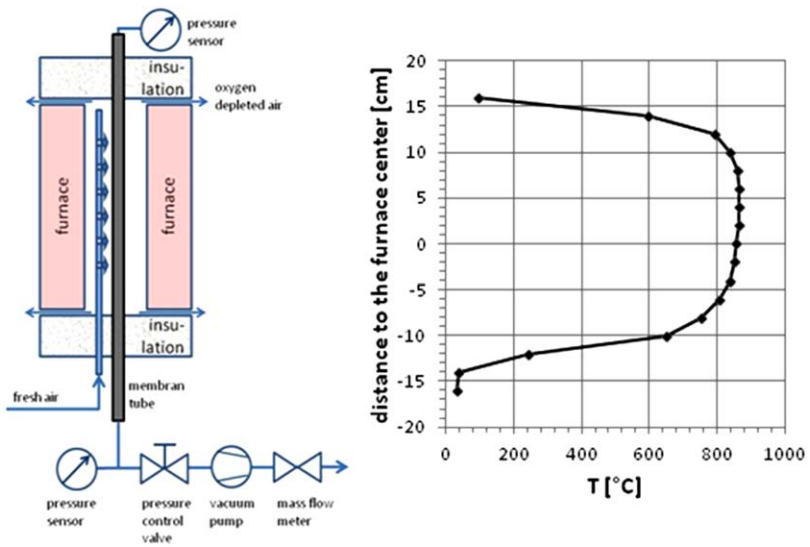

Figure 4. Scheme of the oxygen permeation test bench (left); temperature profile measured inside a membrane tube at 850°C (right).

[Color figure can be viewed in the online issue, which is available at wileyonlinelibrary.com.]

Table 1. Average Pore Size, Open Porosity and Strength of BSCF and BSCF 3Zr Membranes Corresponding Porous Membrane Supports

Material	Content of PMMA beads [wt.-%]	Sintering temperature [°C]	Open porosity [%]	Averaged pore size d_{50} [μm]	Radial bending strength [MPa]
BSCF	–	1130	0.2	0.01	99.6
BSCF	20	1130	41.2	5.7	36.0
BSCF3Zr	–	1130	0.35	0.02	112.8
BSCF3Zr	20	1130	41.3	3.7	20.2

varied from 180 mbar down to the minimal reachable pressure. This total minimal pressure is determined by the interaction of the suction capacity of the vacuum pump (ACP15 by Alcatel) and the total oxygen flux controlled by the membrane type and the temperature. Compressed air was used to realize a constant feed throughput of 10 L (STP)/min at ambient pressure. The feed air was injected into the inner space of the furnace using an alumina tube with small open slits realizing a cross flow of feed air regarding the membrane axis.

The driving force for oxygen permeation $\ln(p_h/p_l)$ was calculated using the vacuum pressure of oxygen (p_l) and the oxygen partial pressure of the feed (p_h). The latter one was calculated from the known value for ambient air of 207 mbar corrected by the oxygen depletion inside the feed. Oxygen depletion in the feed gas was calculated using the measured oxygen flux and the constant feed throughput. The oxygen flux was directly measured after the vacuum pump by a mass flow meter calibrated to pure oxygen at standard conditions (STP: 1013.25 mbar, 273.15 K). Oxygen purity monitored by a calibrated paramagnetic O_2 sensor (Parox 1000, Setnag) was always above 99 vol. %.

Characterization and Results

Microstructure of supports

The influence of the pore forming agent PMMA on microstructure and mechanical strength of the BSCF ceramic was characterized in comparison to conventional monolithic membranes. Table 1 summarizes the results obtained after sintering at the same conditions. The microstructure of sintered porous membrane supports based on BSCF and BSCF3Zr is illustrated by Figures 5 and 6, respectively.

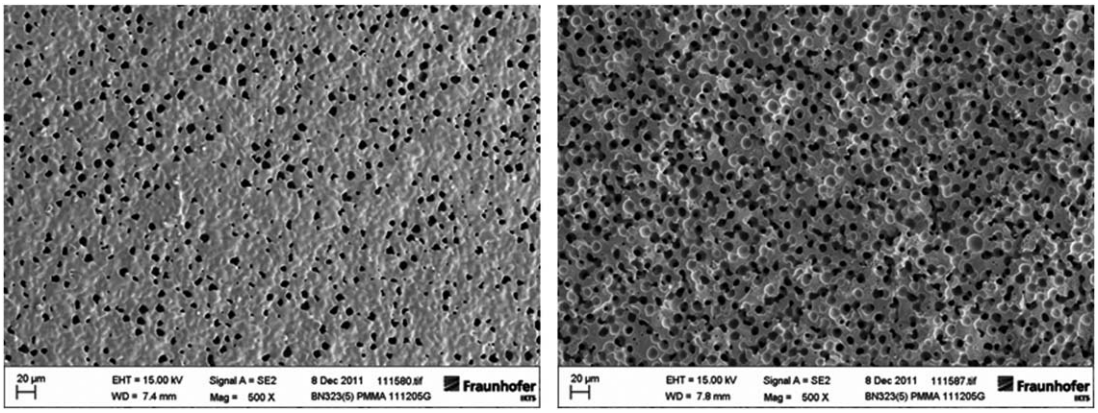

Figure 5. SEM pictures of sintered porous BSCF supports after sintering; left: surface; right: cross section.

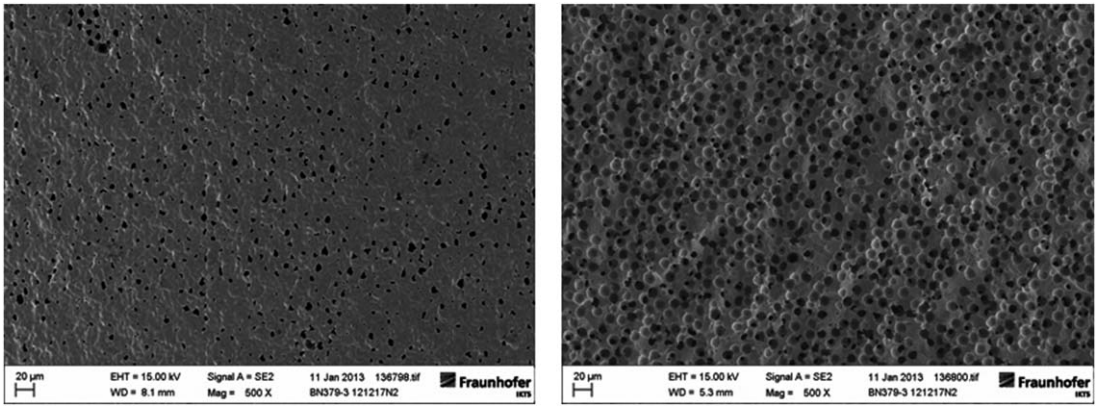

Figure 6. SEM pictures of sintered porous BSCF3Zr supports after sintering; left: surface; right: cross section.

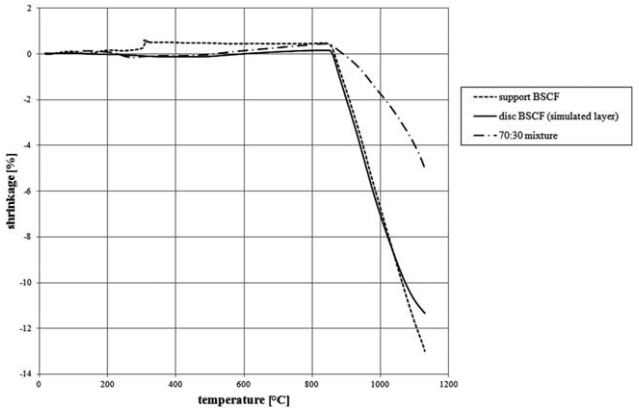

Figure 7. Shrinkage of the PMMA containing BSCF support compared to the disc sample representing the coating layer.

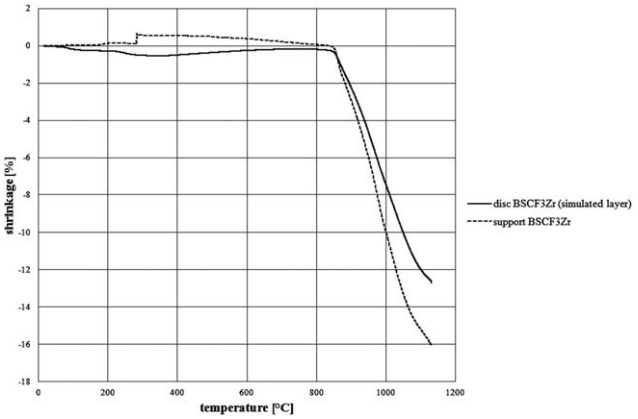

Figure 8. Shrinkage of the PMMA containing BSCF3Zr support compared to the disc sample representing the coating layer.

Dilatometer Measurement. Dilatometric measurements of different samples are shown in Figures 7 and 8 for BSCF and BSCF3Zr, respectively. Obviously, the shrinkage of the support is higher compared to the coating layer represented by the dry compressed discs, especially above 1100°C. This behavior should be accompanied by compressive stress inside the membrane layer during a co-firing sintering step at high temperature compacting the top layer. Nevertheless, the higher content of binder in the real coating slurry could also cause a higher shrinkage of the coating layer compared to the measurements presented.

At a low temperature of $\approx$ 280°C a sharp expansion peak is observed for both support samples indicating the burning out of the pore-forming agent. This is indicated by Figure 7 showing also a measurement on a porous support prepared without pore former using a mixture of 70 vol. % of a coarse powder and 30 vol. % of a fine powder. In this case, the shrinkage is much lower and the sharp peak at 280°C is absent. Using such a porous support with a maximal shrinkage of 3% only, a manufacturing of a dense layer requires a multiple coating as already described.[11,15]

Leakage rate

The coating process was developed and optimized using the correlation between the coating and sintering parameters and the leakage rates measured on the sintered asymmetric membrane tubes. Leakage rates as low as 0.002 ml STP/(cm^2·min) for BSCF and 0.003 mL STP/(cm^2·min) for BSCF3Zr were reached for an optimized coating process.

Membrane Characterization by SEM-Method. SEM pictures of the asymmetric membranes sintered at 1100°C are depicted in Figures 9 and 10. The layer thickness varies from 8 to 10 μm for BSCF and from 20 to 25 μm for BSCF3Zr. Some small closed pores are visible inside the gas-tight separation layer. The grain size visible at the surface varies between 10 and 50 μm.

Oxygen permeation measurements

The oxygen fluxes of monolithic BSCF, asymmetric BSCF and asymmetric BSCF3Zr membrane tubes are shown in Figure 11, Figures 12 and 13, respectively. As expected, the oxygen fluxes observed for the asymmetric membranes were significantly higher compared to the monolithic membranes used as a reference. An improvement factor between 3 and 4 was observed for the asymmetric BSCF3Zr and the BSCF membrane at 900°C and moderate driving forces of $\ln(p_h/p_l) \leq 1$, respectively. The highest oxygen flux of 356 mL STP/min at 900°C was obtained for the asymmetric BSCF membrane. The lower value of 311 mL STP/min for

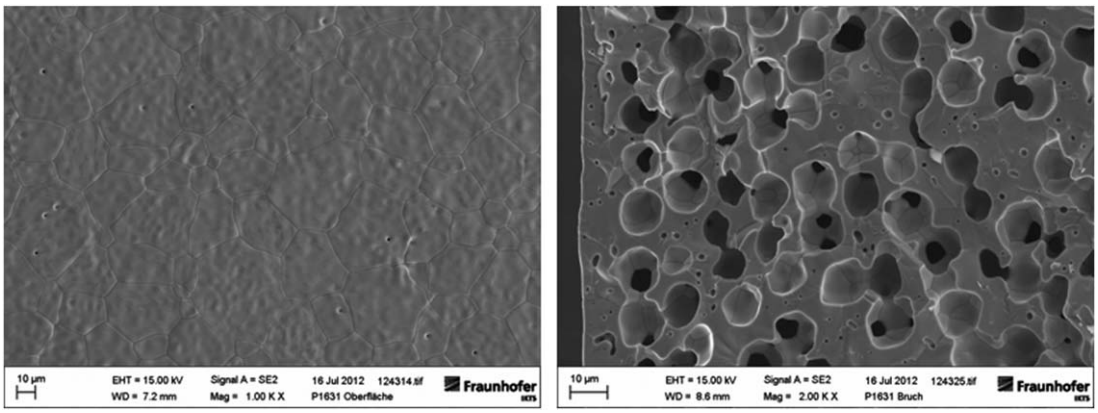

Figure 9. SEM images of the surface and the cross section of an asymmetric BSCF membrane, leakage rate of 0.002 mL STP/(cm^2·min).

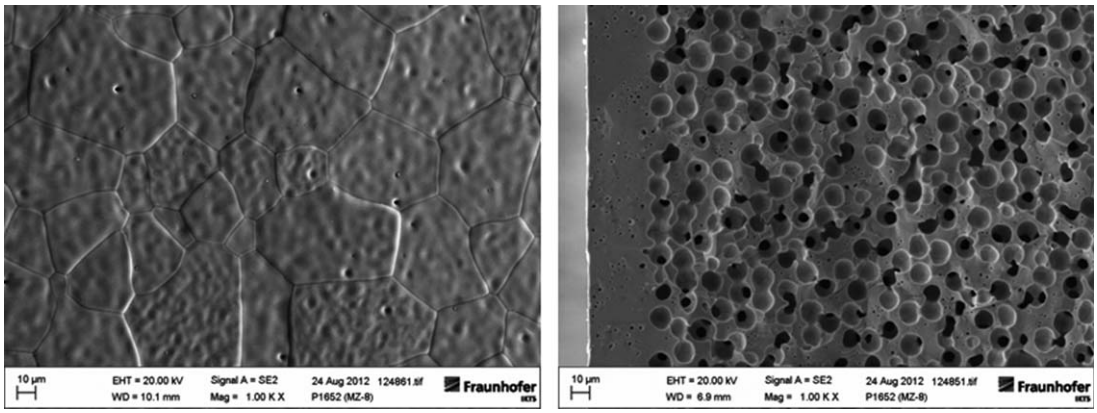

Figure 10. SEM images of the surface and the cross section of an asymmetric BSCF3Zr membrane, leakage rate of 0.07 mL STP/(cm²·min).

the asymmetric BSCF3Zr membrane could be caused by the higher thickness of the top layer. However, the thickness of the membrane top layer is already quite below the critical thickness estimated for BSCF to 50 to 100 μm.[16,17] Therefore, a decrease of the oxygen ion conductivity caused by the Zr doping seems to be more likely. The introduction of Zr^{4+} instead of Co^{3+}/Fe^{3+} decreases the oxygen vacancy concentration and could also affect the mobility of charge carriers and oxygen ions.

The main advantage of Zr doping should be the shifting of the lower temperature limit of the perovskite phase stability range below 800°C [7]. Therefore, a stable oxygen permeation could be also expected for asymmetric BSCF3Zr membranes at 800°C but this was not proven in this work.

Obviously, the oxygen flux increases much less than expected for a transport behavior limited by bulk diffusion according Wagner.[18] This is already visible for the monolithic tube at high-driving forces of $\ln(p_h/p_l) > 2$. Therefore, a limitation of the whole oxygen transport by the surface exchange seems to be likely, especially at high-driving forces or at the entailed low-oxygen partial pressures at the permeate side. Nevertheless, deviations from a linear behavior are much larger for the asymmetric membranes.

High driving forces *in vacuo* operation mode were realized by low-vacuum pressures applied at the permeate side of the membranes. It is well-known that pressure drops in a vacuum system increases exponentially for decreasing vacuum pressures and smaller free diameter of the vacuum piping. Corresponding to the small pore diameter of the porous support used for the asymmetric membranes, the flattening of the O_2 permeation at higher driving forces or smaller vacuum pressures is probably caused by the increasing pressure drop entailed. A comparable behavior was already observed and explained by Schulz et al.[11] for small capillaries.

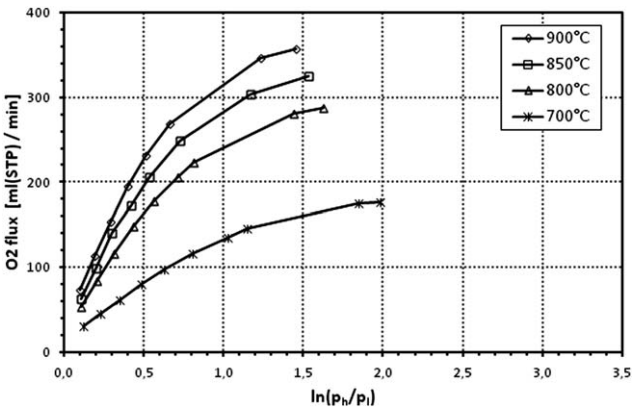

Figure 12. Oxygen flux through an asymmetric BSCF membrane tube.

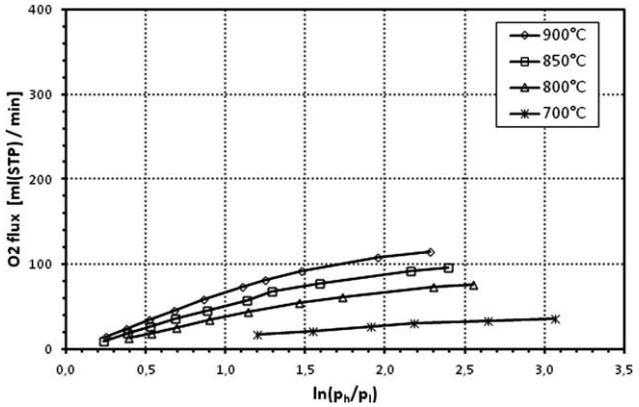

Figure 11. Oxygen flux through a monolithic BSCF membrane tube.

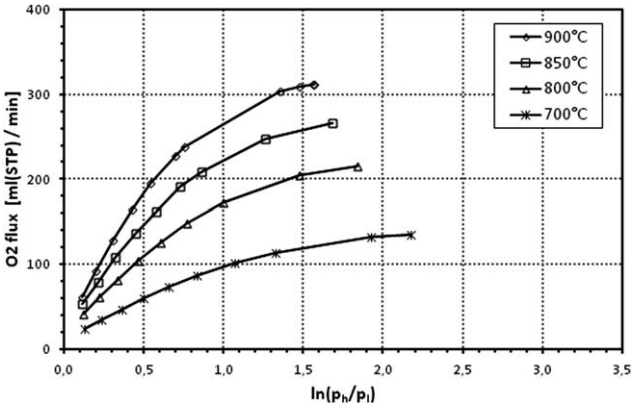

Figure 13. Oxygen flux through an asymmetric BSCF3Zr membrane tube.

Conclusions

The economic benefit of oxygen production using mixed conducting membranes seems to be unquestionable, if the high temperature of an industrial process like combustion or gasification can be used. However, a commercially viable process needs also a sufficient oxygen permeation to limit the capital costs for membrane production. Accordingly, a minimal oxygen permeation of 10 mL STP/(cm^2 · min) was claimed by Bredesen et al.[15,19] Besides, production of small flat asymmetric BSCF membranes should be possible by tape casting[14] or uniaxial pressing,[13] but building-up of large-module stacks seems to be not reasonable because of the high-stress generated inside planar systems.[20] Manufacturing of tubular asymmetric BSCF membranes by using a sintered support required a five-step coating.[13] This way is accompanied with high costs.[9] Correspondingly, membrane production cost varies significantly with membrane design and the membrane area aimed.[9]

A one-step manufacturing technique for long asymmetric BSCF membrane tubes decreases the capital costs of a membrane plant significantly, since the production costs should be only slightly higher compared to monolithic tubes and the oxygen flux is improved by a factor of 3 to 4 at comparable operation conditions. Since the maximal oxygen permeation of 12.0 mL STP/(cm^2 · min) derived from data in Figure 12 outperforms the predicted limit of 10 mL STP/(cm^2 · min),[19] this seems to be an important step forward to an industrial application.

Acknowledgment

The research leading to these results has received funding from the European Commission under the 7th Framework Programme (FP7/2007–2013), grant agreement No. 268165 (HETMOC).

Literature Cited

1. Teraoka Y, Nobunaga T, Yamazoe N. Effect of cation substitution on the oxygen semipermeability of perovskite-type oxides. *Chem Lett*. 1988:503–506.
2. Bouwmeester HJM, Burggraaf AJ. Dense ceramic membranes for oxygen separation. *Fund Inorg Memb Sci Technol*. 1996;4:435–528.
3. Wang H, Wang R, Liang DT, Yang W. Experimental and modeling studies on $Ba_{0.5}Sr_{0.5}Co_{0.8}Fe_{0.2}O_{3-\delta}$ (BSCF) tubular membranes for air separation. *J Memb Sci*. 2004;243(1–2):405–415.
4. Švarcová S, Wiik K, Tolchard J, Bouwmeester HJM, Grande T. Structural instability of cubic perovskite $Ba_xSr_{1-x}Co_{1-y}Fe_yO_{3-\delta}$. *Solid State Ionics*. 2008;178(35-36):1787–1791.
5. Niedrig C, Taufall S, Burriel M, Menesklou W, Wagner SF, Baumann S, Ivers-Tiffèe E. Thermal stability of the cubic phase in $Ba_{0.5}Sr_{0.5}Co_{0.8}Fe_{0.2}O_{3-\delta}$ (BSCF). *Solid State Ionics*. 2011;197(1):25–31.
6. Fang SM, Yoo C, Bouwmeester HJM. Performance and stability of niobium-substituted $Ba_{0.5}Sr_{0.5}Co_{0.8}Fe_{0.2}O_{3-\delta}$ membranes. *Solid State Ionics*. 2011;195(1):1–6.
7. Meng X, Yang N, Meng B, Tan X, Ma Z, Liu S. Zirconium stabilized $Ba_{0.5}Sr_{0.5}(Co_{0.8-x}Zr_x)Fe_{0.2}O_{3-\alpha}$ perovskite hollow fibre membranes for oxygen separation. *Ceramics Int*. 2011;37(7):2701–2709.
8. Repasky J, Anderson L, Stein V, Armstrong P, Foster E. ITM Oxygen technology: scale-up toward clean energy applications. International Pittsburgh Coal Conference 2012; October 15, 2012; Pittsburgh, PA.
9. Kriegel R. Einsatz keramischer BSCF-Membranen in einem transportablen Sauerstoff-Erzeuger. DKG-Handbuch Technische Keramische Werkstoffe. 2010;*Chap* 8.10.1.1:1–46.
10. Kriegel R, Voigt I. Demonstration of oxygen separation with BSCF membranes. 12. Jülicher Werkstoffsymposium; October 5, 2011; Jülich, Germany.
11. Schulz M, Pippardt U, Kiesel L, Ritter K, Kriegel R. Oxygen permeation of various archetypes of oxygen membranes based on BSCF. *AIChE J*. 2012;58(10):3195–3202.
12. Waller D. inventor; Norsk Hydro ASA, 0240 Oslo / NO. Method for manufacturing a membrane. European patent 1156868. February 18, 2000.
13. Kovalevsky AV, Yaremchenko AA, Kolotygin VA, Snijkers FMM, Kharton VV, Buekenhoudt A, Luyten JJ. Oxygen permeability and stability of asymmetric multilayer $Ba_{0.5}Sr_{0.5}Co_{0.8}Fe_{0.2}O_{3-\delta}$ ceramic membranes. Proceedings of the 17th International Conference on Solid State Ionics. 2011;192(1):677–681.
14. Baumann S, Serra JM, Lobera MP, Escolástico S, Schulze-Küppers F, Meulenberg WA. Ultrahigh oxygen permeation flux through supported $Ba_{0.5}Sr_{0.5}Co_{0.8}Fe_{0.2}O_{3-\delta}$ membranes. *J Memb Sci*. 2011;377(1-2):198–205.
15. Böer J, Kiesel L, Pippardt U. Keramische asymmetrische Membranen aus $Ba_{0,5}Sr_{0,5}Co_{0,8}Fe_{0,2}O_{3-\delta}$ zur Sauerstoffseparation. DKG-Jahrestagung; March 22, 2010; Hermsdorf, Germany.
16. Girdauskaite E, Ullmann H, Vashook VV, et al. Oxygen transport properties of $Ba_{0.5}Sr_{0.5}Co_{0.8}Fe_{0.2}O_{3-\delta}$ and $Ca_{0.5}Sr_{0.5}Mn_{0.8}Fe_{0.2}O_{3-x}$ obtained from permeation and conductivity relaxation experiments. *Solid State Ionics*. 2008;179(11-12):385–392.
17. Bucher E, Egger A, Ried P., Sitte W., Holtappels P. Oxygen nonstoichiometry and exchange kinetics of $Ba_{0.5}Sr_{0.5}Co_{0.8}Fe_{0.2}O_{3-\delta}$. *Solid State Ionics*. 2008;(179):1032–1035.
18. Wagner C. Equations for transport in solid oxides and sulfides of transition metals: Progress *Solid State Chem*. 1975;10:3–16.
19. Bredesen RSJ. A technical and economic assessment of membrane reactors for hydrogen and syngas production. Seminar on the Ecological Applications of Innovative Membrane Technology in the Chemical Industry; 1996; Cetraro, Italy.
20. Kriegel R, Schulz M, Ritter K, Kiesel L, Pippardt U, Stahn M, Voigt I. Advanced membrane design for oxygen separation. Efficient Carbon Capture for Coal Power Plants; 2011. Book of extended abstracts.

Manuscript received Jun. 14, 2013, revision received Sept. 20, 2013.